PCCP

Accepted Manuscript

This is an *Accepted Manuscript*, which has been through the Royal Society of Chemistry peer review process and has been accepted for publication.

Accepted Manuscripts are published online shortly after acceptance, before technical editing, formatting and proof reading. Using this free service, authors can make their results available to the community, in citable form, before we publish the edited article. We will replace this *Accepted Manuscript* with the edited and formatted *Advance Article* as soon as it is available.

You can find more information about *Accepted Manuscripts* in the **Information for Authors**.

Please note that technical editing may introduce minor changes to the text and/or graphics, which may alter content. The journal's standard **Terms & Conditions** and the **Ethical guidelines** still apply. In no event shall the Royal Society of Chemistry be held responsible for any errors or omissions in this *Accepted Manuscript* or any consequences arising from the use of any information it contains.

Surface Treatment by Binary Solvents Inducing Crystallization of Small Molecular Donor for Enhanced Photovoltaic Performance

Weihua Zhou[a,b], Yuanpeng Xie[a], Xiaotian Hu[a], Lin Zhang[a], Xiangchuan Meng[a], Yong Zhang[b], Wei Ma*[c], Yiwang Chen*[a,b]

[a]School of Material Science and Engineering/Institute of Polymers, Nanchang University, 999 Xuefu Avenue, Nanchang 330031, China

[b] College of Chemistry/Jiangxi Provincial Key Laboratory of New Energy Chemistry, Nanchang University, 999 Xuefu Avenue, Nanchang 330031, China

[c]State Key Laboratory for Mechanical Behavior of Materials, Xi'an Jiaotong University, 28 Xianning West Rd, Xi'an 710049, China

Corresponding author. Tel.: +86 791 83968703; fax: +86 791 83969561. E-mail: ywchen@ncu.edu.cn (Y. Chen); msewma@mail.xjtu.edu.cn (W. Ma)

Author contributions. Weihua Zhou and Yuanpeng Xie contributed equally to this work.

1

Abstract

The surface treatment of the active layer by the binary solvents composing of methanol (MeOH) and 1-chloronaphthalene (CN) was demonstrated to effectively improve the power conversion efficiency (PCE) from 2.4% to 6.5% for p-DTS(FBTTh$_2$)$_2$:PC$_{71}$BM based small molecular solar cells. The optical property and morphology of p-DTS(FBTTh$_2$)$_2$:PC$_{71}$BM films was carefully investigated. The results indicate that the treatment by MeOH:CN binary solvents could significantly enhance the absorption of the active layer, due to the formation of more p-DTS(FBTTh$_2$)$_2$ nanofibrils associating with higher crystallinity as revealed by atomic force microscopy (AFM) and transmission electron microscopy (TEM). The two-dimensional grazing incidence wide-angle X-ray scattering (GIWAXS) result further demonstrate that the molecular packing of p-DTS(FBTTh$_2$)$_2$ molecules could be strongly enhanced after the treatment by binary solvent. In contrast, the pristine methanol shows of no significant influence on the crystalline structure, phase separation as well as the photovoltaic properties of p-DTS(FBTTh$_2$)$_2$:PC$_{71}$BM system, showing that CN solvent plays the main role in inducing the crystallization of p-DTS(FBTTh$_2$)$_2$ molecules.

Keywords: crystallization; grazing incidence wide-angle X-ray scattering; binary solvents; organic solar cells

1. Introduction

Solution-processed organic solar cells (OSCs) shows of great potential as a competitive technology of green energy, attributing to the advantages of low cost, light weight, and high mechanical flexibility.[1] Due to the significant improvements in active layer, device structure, and fabricating techniques, power conversion efficiency (PCE) over 10% have been achieved for polymer solar cells.[2] Recently, prominent efficiency with 10.08% has also been achieved for small molecular solar cells.[3] The small molecular solar cells demonstrate many prominent advantages as compared with polymer solar cells in terms of ease of purification, discrete molecular weight, small batch-to-batch variation, and high open-circuit voltage (V_{oc}).[4]

The most studied small molecular donors include the oligothiophene derivatives with an acceptor-donor-acceptor (A-D-A) structure reported by Chen's group[3,5-15] and the dithienosilole (DTS) based molecules reported by Bazan's group.[16-21] Although the corresponding solar cells exhibited relatively high PCE, the major challenge for them is to simultaneously enhance the molecular order for better charge carrier mobility, and to restrict the domain size due to limited exciton diffusion length (10-20 nm).[22-24] Strategies simultaneously to enhance molecular order and restrict domain size have been reported, including thermal annealing,[5] solvent vapor annealing[25] solvent additives and polymer additives,[21] etc.

All the above mentioned methods aimed to reconstruct nanomorphology for enhanced photovoltaic properties. Recently, a top-down approach applying to reconstruct the nanophase of the active layer was reported, via the simple rinsing treatment by a solvent mixture comprising a trace of solvent additive such as 1,8-diiodooctane (DIO) or 1-chloronaphthalene (CN) and most non-polar buffer solvents.[26] Additionally, the treatment of active layer with polar solvents such as alcohols could considerably enhance the PCE of polymer solar cells before deposition of metal electrodes, due to the optimization of morphology of the active layers and/or change the interface between the active layer and the buffer layer. Park *et al*. found that the optimal phase

3

separation in the poly(3-hexylthiophene):[6,6]-phenyl-C_{61}-butyric acid methyl ester (P3HT:PCBM) films could be obtained after treating by ethanol, arising from the formation of PCBM aggregates rather than from changes in the crystalline ordering of P3HT.[27] Similarly, Yang *et al.* found that the lateral and vertical nanoscale phase separation of P3HT:PCBM films could be optimized via soaking by solvents composing of methanol (MeOH) and carbon disulfide (CS_2), showing of enhanced PCE. The CS_2 may activate the chain motion of P3HT and the diffusion of PCBM molecules laterally and vertically.[28] It is concluded that the surface treatment of the active layer by alcohols such as MeOH or the binary solvents is demonstrated to be effective in optimizing morphology of active layer and improving performance of polymer solar cells. Therefore, the method of surface treatment by MeOH and its binary solvent containing CN additive might also be useful for the small molecular system, via optimizing the nanomorphology for enhanced device performance.

As the 7,7'-(4,4-bis(2-ethylhexyl)-4H-silolo[3,2-b:4,5-b']dithiophene-2,6-diyl)bis(6-fluoro-4-(5'-hexyl-[2,2'-bithiophen]-5-yl)benzo[c][1,2,5]thiadiazole):[6,6]-phenyl-C_{71}-butyric acid methyl ester (*p*-DTS(FBTTh$_2$)$_2$:PC$_{71}$BM) system is concerned, the methanol is supposed to be able to induce aggregation of PC$_{71}$BM molecules into larger clusters. Moreover, the crystallization of donor *p*-DTS(FBTTh$_2$)$_2$ molecules into interconnected nanofibrils should be vital to enhance the charge carrier transportation and device efficiency. The solvent treatment by methanol may be unable to induce the crystallization of *p*-DTS(FBTTh$_2$)$_2$ molecules, and the 1-chloronaphthalene (CN) solvent might be facilitating the molecular packing of *p*-DTS(FBTTh$_2$)$_2$ molecules. Therefore, the binary solvent composing of MeOH and CN is supposed to be able to reconstruct the nanophase of *p*-DTS(FBTTh$_2$)$_2$:PC$_{71}$BM system via optimizing the ratio of CN to MeOH.

In this study, the binary solvent of CN and MeOH was used to soak the *p*-DTS(FBTTh$_2$)$_2$:PC$_{71}$BM films via wetting and quick spin, leading to a significant

improvement of PCE from 2.4% to 6.5%. The influence of the composition of binary solvent on the phase separation of active layer and crystalline structure of p-DTS(FBTTh$_2$)$_2$ was carefully investigated. The MeOH solvent is found to show of no significant influence on the crystalline structure of p-DTS(FBTTh$_2$)$_2$ and the morphology of the films. The binary solvent is demonstrated to induce the crystallization of p-DTS(FBTTh$_2$)$_2$ into nanofibrils, optimizing the nanomorphology of the active layer for enhanced photovoltaic properties.

2. Experimental section

2.1 Materials

p-DTS(FBTTh$_2$)$_2$ was purchased from 1-Material Chemscitech Inc. PC$_{71}$BM was purchased from Nano-C Inc. 1-chloronaphthalene (CN) and methanol (MeOH) was supplied by Sigma Aldrich.

2.2 Device fabrication

Solution-processed small molecular solar cells with conventional device architecture of ITO/ZnO/p-DTS(FBTTh$_2$)$_2$/PC$_{71}$BM/MoO$_3$/Ag were fabricated according to the following procedure. The ITO-coated glass substrates were firstly cleaned by ultrasonic treatment in detergent deionized water, acetone and isopropyl alcohol for 30 minutes each. After treating with UV/ozone for 20 min, ZnO precursor solution was spin-coated at 4000 rpm and the ZnO layer was generated at 220 °C in ambient atmosphere. Active layers were spun at 1750 rpm from solution of p-DTS(FBTTh$_2$)$_2$:PC$_{71}$BM at weight ratio of 3:2 and an overall concentration of 35 mg/mL. Solution was heated for 15 min at 90 °C prior to cast. The obtained films were allowed to dry for 30 min and then heat to 70 °C for 10 min under inert atmosphere to drive off residual solvent. Then, a specific binary solvent containing a few traces of CN and most MeOH solvent was dropped onto the active layer surface via 15 seconds wetting treatment and spinning at 3600 rpm. The MoO$_3$ were deposited by sequentially thermal evaporation of 7 nm, followed by 90 nm of Ag.

2.3 Characterizations

Current-voltage (J-V) characteristics were characterized using Keithley 2400. The current was measured in the dark and under 100 mW·cm^{-2} simulated AM 1.5 G irradiation (Abet Solar Simulator Sun2000). All the measurements were performed under ambient atmosphere at room temperature. The scan range is from 0 V to 1 V, and 6.7 mV for each step. The hole-only diodes were fabricated in device geometry similar to solar cell devices, except that ZnO was replaced by PEDOT:PSS. The J-V characteristics of the diodes show of an excellent fit to the Mott–Gurney relation for

space charge limited current (SCLC). The ultraviolet-visible (UV) spectra of the specimens were recorded by a PerkinElmer Lambda 750 spectrophotometer. Atomic force microscopy (AFM) using a Digital Instrumental Nanoscope 31 was operated in the tapping mode. Samples for transmission electron microscopy (TEM) observation were prepared by spin-coating PEDOT:PSS on the ITO glass at 2000 rpm and drying at ambient atmosphere. Then, the active layers were spun at 1750 rpm, followed by drying for 30 min and thermal annealing at 70 °C for 10 min. After surface treatment by MeOH or MeOH:CN solvents, the specimen was drying for 30 min. The films were then floated off the substrate in deionized water and collected on a copper mesh grid. Grazing incidence wide-angle X-ray scattering (GIWAXS) measurement was performed at beamline 7.3.3 at the Advanced Light Source (ALS), Berkeley, USA. Samples were prepared on Si substrates with a thin ZnO layer by using identical blend solutions as those used in devices. The incident angle was 0.14°, which maximized the scattering intensity from the samples. The scattered X-rays were detected by using a Dectris Pilatus 2M photon counting detector.

3. Results and discussion

The chemical structure of p-DTS(FBTTh$_2$)$_2$ is shown in **Figure 1a**, and Bazan's group have extensively studied the crystalline structure, as well as the morphology evolution of p-DTS(FBTTh$_2$)$_2$:PC$_{71}$BM films upon thermal annealing,[16] incorporation of DIO additive[19, 20] and polystyrene[21] and so on. To induce the crystallization of p-DTS(FBTTh$_2$)$_2$ into ordered nanofibrils may enhance the domain purity, leading to the improvement of photovoltaic properties. In order to explore the effect of surface treatment by solvents, the corresponding absorption behaviors, morphology and photovoltaic properties of the films were studied.

The inverted structure of organic photovoltaic cell (OPV) devices is known for its better stability as compared with the traditional OPV devices. In this article, the device with the structure of ITO/ZnO/p-DTS(FBTTh$_2$)$_2$:PC$_{71}$BM/MoO$_3$/Ag was fabricated, and the corresponding current-density-voltage (J-V) characteristics under one sun (simulated AM 1.5 G irradiation at 100 mW/cm^2) are presented in **Figure 1b**. The corresponding device parameters are shown in **Table 1**. It is observed that the shape of the J-V curves is strongly dependent on the volume ratio of MeOH with CN. For the pristine specimen without solvent treatment, the short-circuit current (J_{sc}) of 8.53 mA/cm^2, open-circuit voltage (V_{oc}) of 0.78 V, fill factor (FF) of 36.4 % and PCE of 2.4 % are noticed. After treating by the MeOH solvent, the above parameters keep almost constant, without significant change. It is believed that MeOH solvent shows of no influence on the device performance. However, the J_{sc} and FF values significantly increase to 10.34 mA/cm^2 and 56.9% after treating by the binary solvent (MeOH:CN=99.5:0.5, v/v), respectively, resulting in an improved PCE of 4.5 %. Further increase of CN volume ratio (MeOH:CN=98:2, v/v) eventually leads to the highest PCE of 6.50 % with a J_{sc} of 11.86 mA/cm^2, V_{oc} of 0.79 V and FF of 69.0 %. At higher CN volume ratio (MeOH:CN=95:5, v/v), the parameters including J_{sc} and FF of the devices obviously reduce to 10.20 mA/cm^2 and 49.6 %, showing of a much lower PCE of 3.87 %.

In order to explore and understand the effect of MeOH:CN binary solvent on the optical properties of the films, the corresponding UV-visible absorption spectra are shown in **Figure 1c**. The pristine p-DTS(FBTTh$_2$)$_2$:PC$_{71}$BM film shows obvious absorption between 400 nm and 750 nm, with two prominent absorption peaks at 620 nm and 670 nm. By the MeOH solvent treatment, the absorption coefficient of the specimen shows of no serious change. However, after treating by the binary solvents, the absorption coefficient of the absorption peaks significantly increases. As reported, the absorption peak at 670 nm is contributed to the vibronic structure of p-DTS(FBTTh$_2$)$_2$, suggesting that the molecular ordering is enhanced.[16] It indicates that the surface treatment by binary solvents might facilitate the crystallization of p-DTS(FBTTh$_2$)$_2$, enhancing the π-π stacking. It is noted that the specimen treated by MeOH:CN (98:2) solvent exhibits the maximal absorption coefficient as compared with the other specimens.

Dark current is shown in **Figure S1**. The bias ranges from -2 V to 2 V, and the negative bias represents the leakage current. [29] There is obvious leakage current at the negative bias in the pristine device, whereas the leakage current of the device decreases after treating by the binary solvents. Especially, the leakage current reduces about 30-fold at -2 V for the specimen after treating by the MeOH:CN (98:2) solvent. The rectification factor of approximately 50 (from -2 V to 2 V) is observed for the pristine device, whereas the rectification factor over 1000 (from -2 V to 2 V) is noticed for the specimen after treating by the MeOH:CN (98:2) solvent.

Charge carrier mobilities in the films have a crucial effect on the performance of the solar cells. To gain insight into how the performance of p-DTS(FBTTh$_2$)$_2$:PC$_{71}$BM based device is influenced by the surface solvent treatments, the hole mobilities of the specimens were measured using the space charge limited current (SCLC) model (**Figure 1d**). The hole mobility of the pristine specimen is 6.8×10^{-5} cm^{2}V^{-1}s^{-1}, which is comparable to the result reported previously.[21] After treating by MeOH, the hole mobility drops to 4.0×10^{-5} cm^{2}V^{-1}s^{-1}, due to the isolated island structure as shown in

AFM images. After surface treatment by MeOH:CN (98:2) solvent, the hole mobility is greatly improved to 5.98×10^{-4} cm^2 V^{-1} s^{-1}, which is almost one order of magnitude as compared with the pristine specimen. The enhancement of hole mobility is mainly attributed to the crystallization of p-DTS(FBTTh$_2$)$_2$ as revealed by the UV analysis.

The photovoltaic performance of the device is believed to be partly determined by the morphology of active layer. It is well-known that a nanoscale phase separation and bicontinuous interpenetrating network in the active layer is necessary to efficiently separate the exciton and form percolating channels for the transport of both holes and electrons.[30] The surface morphology of the p-DTS(FBTTh$_2$)$_2$:PC$_{71}$BM without and with MeOH:CN treatment was characterized using atomic force microscopy (AFM). Surface topography and phase images were taken for different films as shown in **Figure 2 and Figure S2**. The pristine p-DTS(FBTTh$_2$)$_2$:PC$_{71}$BM film is smooth and uniform, with a root-means-square (RMS) roughness of 0.504 nm. After treating by MeOH solvent, an abundant island structure is observed, with the RMS value of 1.24 nm. The island structure might be attributing to the formation of PCBM clusters induced by MeOH as reported in the P3HT:PCBM system.[27] By the treatment of MeOH:CN binary solvents, the surface morphology of the films experiences significant change, accompanied by increase of RMS values. The phase-separated morphology for the specimen treating by MeOH:CN (99.5:0.5) solvent becomes more obviously in contrast to the pristine specimen without solvent treatment. As the CN volume ratio increasing, the bright regions become more dominant, and the domain size also increases. As the specimen after treating by MeOH:CN (98:2) solvent is concerned, the bright domains grow to bigger size. Additionally, the RMS value is 12.71 nm, which is the highest among all the specimens. Further increase of the CN volume ratio eventually leads to the decrease of bright domain sizes, as well as the reduction of RMS value to 9.57 nm. It is suggested that too much CN is not beneficial for the active layer to form optimized morphology.

Due to the fact that AFM only provides the information of film surface morphology,

the bulk morphology of the films is further characterized by transmission electron microscopy (TEM) to understand the origin of the enhanced performance (**Figure 3**). For the pristine *p*-DTS(FBTTh$_2$)$_2$:PC$_{71}$BM film without solvent treatment, the homogeneous morphology without significant phase separation could be observed, indicating that the donor and acceptor molecules are well mixed. Through the treatment with MeOH, the homogeneous morphology of the film shows of no obvious change except for a small amount of black aggregates attributing to PC$_{71}$BM aggregates.[31] In contrast, the film treated by MeOH:CN (99.5:0.5) presents a mass of fibril structure of *p*-DTS(FBTTh$_2$)$_2$ crystallites with characteristic widths of about 5-10 nm and lengths of hundreds of nanometers, which ultimately leads to the formation of necessary pathways for charge transport to the electrodes. Further increasing of CN volume ratio in the binary solvent eventually leads to the appearance of *p*-DTS(FBTTh$_2$)$_2$ crystallites in larger size. By increasing of CN content, the number of fibrils decreases, but the width becomes larger. For the specimen treating by MeOH:CN (98:2) solvent, the fibril in the width up to 30 nm could be discerned, which is consistent with the result observed by AFM. Further increase of the volume fraction of CN in the binary solvent leads to the disappearance of evident *p*-DTS(FBTTh$_2$)$_2$ fibrils. For the specimen treating by MeOH:CN (95:5) solvent, the less obvious fibrils could be discerned from the TEM image, implying that the excess of CN solvent may dissolve the *p*-DTS(FBTTh$_2$)$_2$ fibrils.

Cross-sectional TEM was further carried out on the pristine *p*-DTS(FBTTh$_2$)$_2$:PC$_{71}$BM film (**Figure 4a**) and film after MeOH:CN (98:2) solvent treatment (**Figure 4b**). It is observed that the thickness of active layer decreases from 83 nm to 72 nm after the binary solvent treatment, indicating that some of the component in the active layer might be washed. According to the selected area electron diffraction (SAED) pattern (**Figure 4c** and **Figure 4d**), the appearance of more diffraction spots in the image illustrates that the sample after solvent treatment is more crystalline than the pristine specimen.

In order to understand how the solvent treatment influence the corresponding crystalline structure of p-DTS(FBTTh$_2$)$_2$, the two-dimensional grazing-incidence wide-angle X-ray scattering (GIWAXS) technique was used to obtain high-resolution scattering profiles, and the corresponding parameters of diffraction signals are list in **Table S1**. As shown in **Figure 5**, the diffraction patterns of pristine p-DTS(FBTTh$_2$)$_2$:PC$_{71}$BM specimen and the specimen after treating by methanol seem to be similar, implying that the methanol shows of no influence on the crystalline structure of the p-DTS(FBTTh$_2$)$_2$. For the pristine specimen is concerned, a series of weak peaks at lower q values appear in the out-of-plane direction. The relatively obvious peak at $q \approx 0.31$ Å^{-1} corresponds to a distance of 2.02 nm in real space, which is typically associated with alkyl stacking (100). The weaker reflections at $q \approx 0.52$ Å^{-1} and 0.82 Å^{-1} could also be observed which are preferentially oriented out-of-plane and are assigned to the second (200) and third (300) order reflections from the alkyl stacking. A weak out-of-plane reflection at $q \approx 1.72$ Å^{-1} corresponds to a real-space distance of 3.65 Å and is attributing to intermolecular π-stacking (010) of the conjugated backbones. Additionally, the in-plane reflection at $q \approx 1.72$ Å^{-1} could also be noticed, indicating that most of the p-DTS(FBTTh$_2$)$_2$ molecules tend to adopt both of edge-on and face-on structure. After the treatment by the MeOH:CN (98:2) solvent, the scattering profiles become stronger and more obvious. An intense out-of-plane reflection at $q \approx 0.28$ Å^{-1} corresponds to a distance of 2.24 nm in real space, associating with the alkyl stacking (100). The position of the reflection shifts to lower q value as compared with the pristine specimen. Moreover, the second and third order reflections are also stronger than those of the pristine specimen, with the position of reflection shifting to higher q values of 0.58 Å^{-1} and 0.85 Å^{-1}. It is indicated that the treatment by binary solvent obviously affect the crystalline structure of p-DTS(FBTTh$_2$)$_2$. The out-of-plane and in-plane reflection at $q = 1.72$ Å^{-1} could be observed, illustrating that the p-DTS(FBTTh$_2$)$_2$ adopts both of the edge-on and face-on structure. The isotropy of the reflection shows that there are some population p-DTS(FBTTh$_2$)$_2$ crystals oriented in all directions within the film.

As a more quantitative measure, we can calculate the crystal correlation length (CCL) which reflects the extent of order in crystalline lattice and increases with the crystallite size. Then, the Scherrer equation[32] was used to estimate the CCL values from the peak breadths, and the corresponding data is illustrating in **Table 2**. The CCL value of the (100) reflection for pristine p-DTS(FBTTh$_2$)$_2$:PC$_{71}$BM specimen is calculated to be about 17.1 nm. The values for the specimens after methanol and MeOH:CN (98:2) treatment are 17.6 nm and 25.0 nm, respectively. Moreover, the CCL values of the (010) reflection are calculated to be 8.5 nm, 8.5 nm and 15.5 nm for the pristine specimen, specimen after methanol or MeOH:CN (98:2) treatment, respectively. The above results indicate that the treatment by binary solvent obviously induce the crystallization of p-DTS(FBTTh$_2$)$_2$ molecules. The enhancement of the absorption and photovoltaic properties of the p-DTS(FBTTh$_2$)$_2$:PC$_{71}$BM specimen after treating by MeOH:CN (98:2) solvent is mainly originating from the formation of more perfect p-DTS(FBTTh$_2$)$_2$ crystallites.

Conclusions

The surface treatment by binary solvent composing of MeOH and CN was demonstrated to significantly enhance the PCE of p-DTS(FBTTh$_2$)$_2$:PCBM system from 2.4% to 6.5%, associating with the significant improvement of hole mobility. However, the MeOH solvent treatment was found to have no obvious influence on the photovoltaic property of the p-DTS(FBTTh$_2$)$_2$:PCBM system. The UV-vis result indicated that the treatment by MeOH:CN (98:2) solvent may enhance the absorption of p-DTS(FBTTh$_2$)$_2$:PCBM films, due to the improved molecular ordering for p-DTS(FBTTh$_2$)$_2$ molecules. The binary solvent treatment could increase the RMS value of the p-DTS(FBTTh$_2$)$_2$:PCBM films from 0.504 nm to 12.71 nm, accompanied by the formation of p-DTS(FBTTh$_2$)$_2$ crystals in larger size as revealed by AFM observation. The TEM result further indicated that the treatment by MeOH showed of no obvious influence on the film morphology, while the treatment by binary solvent could induce the formation of better nanofibrils network, leading to higher crystallinity of p-DTS(FBTTh$_2$)$_2$ crystallites as demonstrated by SAED analysis. The GIWAXS result revealed that the treatment by MeOH:CN binary solvent could significantly induce the crystallization of p-DTS(FBTTh$_2$)$_2$ molecules, showing of larger CCL value as compared with the pristine p-DTS(FBTTh$_2$)$_2$:PCBM specimen. The method could be applicable for the other small molecular systems for the enhancement of the photovoltaic performance.

Supporting Information

The dark current-voltage (*J-V*) characteristics, AFM phase images and parameters of the diffraction signals for GIWAXS measuremnt are in Supporting Information. This information is available free of charge via the Internet at http://pubs.rsc.org.

References

1. R. F. Service, *Science*, 2011, **332**, 293.

2. Y. H. Liu, J. B. Zhao, Z. K. Li, C. Mu, W. Ma, H. W. Hu, K. Jiang, H. R. Lin, H. Ade, H. Yan, *Nat. Commun.*, 2014, **5**, 5293.

3. B. Kan, M. Li, Q. Zhang, F. Liu, X. Wan, Y. Wang, W. Ni, G. Long, X. Yang, H. Feng, Y. Zuo, M. Zhang, F. Huang, Y. Cao, T. P. Russell, Y. Chen, *J. Am. Chem. Soc.*, 2015, **137**, 3886-3893.

4. Y. Chen, X. Wan, G. Long, *Acc. Chem. Res.*, 2013, **46**, 2645-2655.

5. Y. Liu, J. Zhou, X. Wan, Y. Chen, *Tetrahedron*, 2009, **65**, 5209-5215.

6. Y. Liu, X. Wan, B. Yin, J. Zhou, G. Long, S. Yin, Y. Chen, *J. Mater. Chem.*, 2010, **20**, 2464-2468.

7. Y. Liu, X. Wan, F. Wang, J. Zhou, G. Long, J. Tian, J. You, Y. Yang, Y. Chen, *Adv. Energy Mater.*, 2011, **1**, 771-775.

8. Y. Liu, X. Wan, F. Wang, J. Zhou, G. Long, J. Tian, Y. Chen, *Adv. Mater*. 2011, **23**, 5387-5391.

9. J. Zhou, X. Wan, Y. Liu, Y. Zuo, Z. Li, G. He, G. Long, W. Ni, C. Li, X. Su, Y. Chen, *J. Am. Chem. Soc.*, 2012, **134**, 16345-16351.

10. G. He, Z. Li, X. Wan, Y. Liu, J. Zhou, G. Long, M. Zhang, Y. Chen., *J. Mater. Chem.*, 2012, **22**, 9173-9180.

11. Z. Li, G. He, X. Wan, Y. Liu, J. Zhou, G. Long, Y. Zuo, M. Zhang, Y. Chen, *Adv. Eng. Mater.*, 2012, **2**, 74-77.

12. G. He, Z. Li, X. Wan, J. Zhou, G. Long, S. Zhang, M. Zhang, Y. Chen. *J. Mater. Chem. A*, 2013, **1**, 1801-1809.

13. J. Zhou, Y. Zuo, X. Wan, G. Long, Q. Zhang, W. Ni, Y. Liu, Z. Li, G. He, C. Li, B. Kan, M. Li, Y. Chen, *J. Am. Chem. Soc.*, 2013, **135**, 8484-8487.

14. B. Kan, Q. Zhang, M. Li, X. Wan, W. Ni, G. Long, Y. Wang, X. Yang, H. Feng, Y. Chen. *J. Am. Chem. Soc.*, 2014, **136**, 15529-15532.

15. Q. Zhang, B. Kan, F. Liu, G. Long, X. Wan, X. Chen, Y. Zuo, W. Ni, H. Zhang, M. Li, Z. Hu, F. Huang, Y. Cao, Z. Liang, M. Zhang, T. P. Russell, Y. Chen, *Nat. Photonics*, 2015, **9**, 35-41.

16. T. S. van der Poll, J. A. Love, T. Q. Nguyen, G. C. Bazan, *Adv. Mater*. 2012, **24**,

3646-3649.

17.   Y. Sun, G. C. Welch, W. L. Leong, C. J. Takacs, G. C. Bazan, A. J. Heeger. *Nat. Mater.*, 2012, **11**, 44-48.

18.   A. K. K. Kyaw, D. H. Wang, V. Gupta, W. L. Leong, L. Ke, G. C. Bazan, A. J. Heeger, *ACS Nano*, 2013, **7**, 4569-4577.

19.   J. A. Love, C. M. Proctor, J. Liu, C. J. Takacs, A. Sharenko, T. S. van der Poll, A. J. Heeger, G. C. Bazan, T. Q. Nguyen, *Adv. Funct. Mater.*, 2013, **23**, 5019-5026.

20.   L. A. Perez, K. W. Chou, J. A. Love, T. S. van der Poll, D. M. Smilgies, T. Q. Nguyen, E. J. Kramer, A. Amassian, G. C. Bazan, *Adv. Mater.*, 2013, **25**, 6380-6384.

21.   Y. Huang, W. Wen, S. Mukherjee, H. Ade, E. J. Kramer, G. C. Bazan, *Adv. Mater.*, 2014, **26**, 4168-4172.

22.   K. Sun, Z. Xiao, E. Hanssen, M. F. G. Klein, H. H. Dam, M. Pfaff, D. Gerthsen, W. W. H. Wong, D. J. Jones. *J. Mater. Chem. A*, 2014, **2**, 9048-9054.

23.   P. Zhang, C. Li, Y. Li, X. Yang, L. Chen, B. Xu, W. Tian, Y. Tu, *Chem. Commun.* 2013, **49**, 4917-4919.

24.   Y. Zhao, G. Xu, X. Guo, Y. Xia, C. Cui, M. Zhang, B. Song, Y. Li, Y. Li. *J. Mater. Chem. A*, 2015, **3**, 17991-18000.

25.   K. Sun, Z. Xiao, S. Lu, W. Zajaczkowski, W. Pisula, E. Hanssen, J. M. White, R. M. Williamson, J. Subbiah, J. Ouyang, A. B. Holmes, W. W. H. Wong, D. J. Jones, *Nat. Mater.*, DOI: 10.1038/ncomms7013.

26.   J. Kong, I. W. Hwang, K. Lee, *Adv. Mater.*, 2014, **26**, 6275-6283.

27.   S. Nam, J. Jang, H. Cha, J. Hwang, T. K. An, S. Park, C. E. Park, *J. Mater. Chem.*, 2012, **22**, 5543-5549.

28.   H. Li, H. Tang, L. Li, W. Xu, X. Zhao, X. Yang, *J. Mater. Chem.*, 2011, **21**, 6563-6568.

29.   A. K. K. Kyaw, D. H. Wang, D. Wynands, J. Zhang, T. Q. Nguyen, G. C. Bazan, A. J. Heeger, *Nano Lett.*, 2013, **13**: 3796-3801.

30.   Y. Liu, C. C. Chen, Z. Hong, J. Gao, Y. Yang, H. Zhou, L. Dou, G. Li, Y. Yang, *Sci. Rep.*, 2013, **3**, 3356.

31.   H. Wan, F. Liu, L. Bu, J. Gao, C. Wang, W. Wei, T. P. Russell, *Adv. Mater.*, 2013, **25**, 6519-6525.

32.   A. Patterson, *Phys*. *Rev*., 1939, **56**, 978-982.

33.   A. Hexemer, W. Bras, J. Glossinger, E. Schaible, E. Gann, R. Kirian, A. MacDowell, M. Church, B. Ride, H. Padmore, *J*. *Phys*. *Conf*. *Ser*., 2010, **247**, 012007.
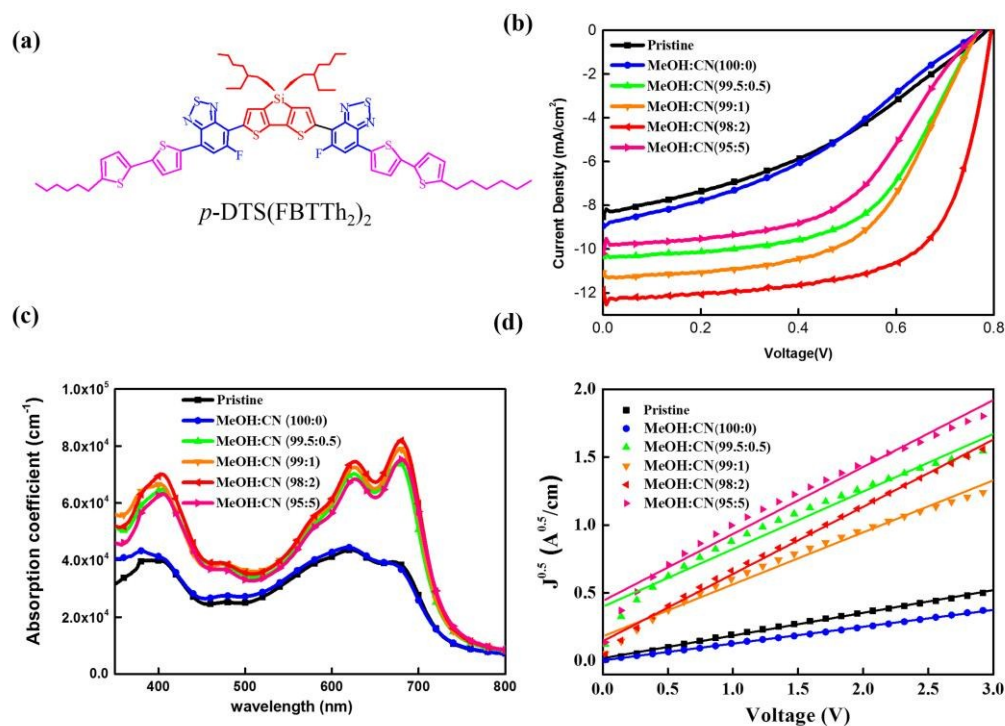
Figure 1 (a) Molecular structure of p-DTS(FBTTh$_2$)$_2$, (b) Current-voltage (J-V) characteristics: current density of molecular solar cells based on p-DTS(FBTTh$_2$)$_2$:PC$_{71}$BM samples without or with solvent treatment, (c) UV-vis absorbance of the p-DTS(FBTTh$_2$)$_2$:PC$_{71}$BM films spun cast on ITO glass without and with solvent treatment, the processing conditions are similar to those used to fabricate the thin-film devices, (d) $J^{0.5}$-V characteristics of hole mobilities (μ_h) using space charge limited current (SCLC) modeling measured at ambient temperature.
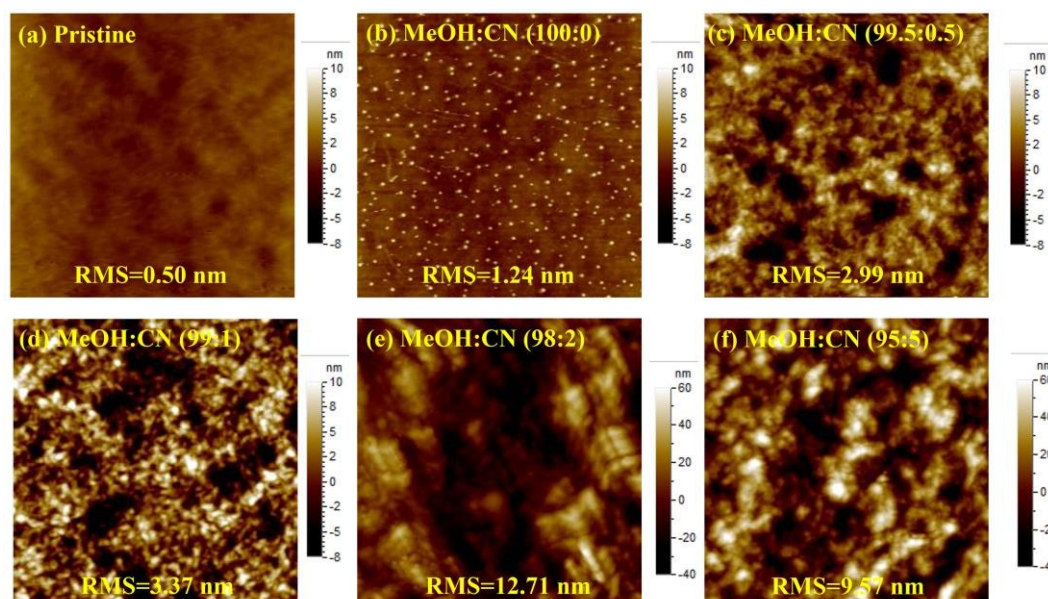
Figure 2 Atomic force microscope (AFM) topography images of (a) pristine p-DTS(FBTTh$_2$)$_2$:PC$_{71}$BM film, and films after treating by binary solvents of (b) MeOH:CN (100:0), (c) MeOH:CN (99.5:0.5), (d) MeOH:CN (99:1), (e) MeOH:CN (98:2) and (f) MeOH:CN (95:5), respectively.
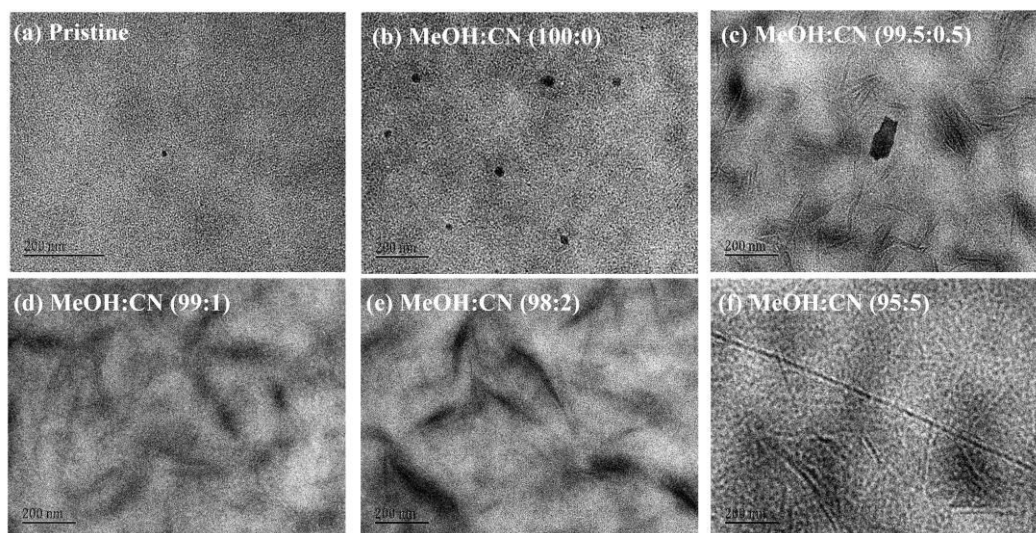
Figure 3 Transmission electron microscope (TEM) images of (a) pristine
p-DTS(FBTTh$_2$)$_2$:PC$_{71}$BM film, and films after treating by binary solvents of (b)
MeOH:CN (100:0), (c) MeOH:CN (99.5:0.5), (d) MeOH:CN (99:1), (e) MeOH:CN
(98:2) and (f) MeOH:CN (95:5), respectively.
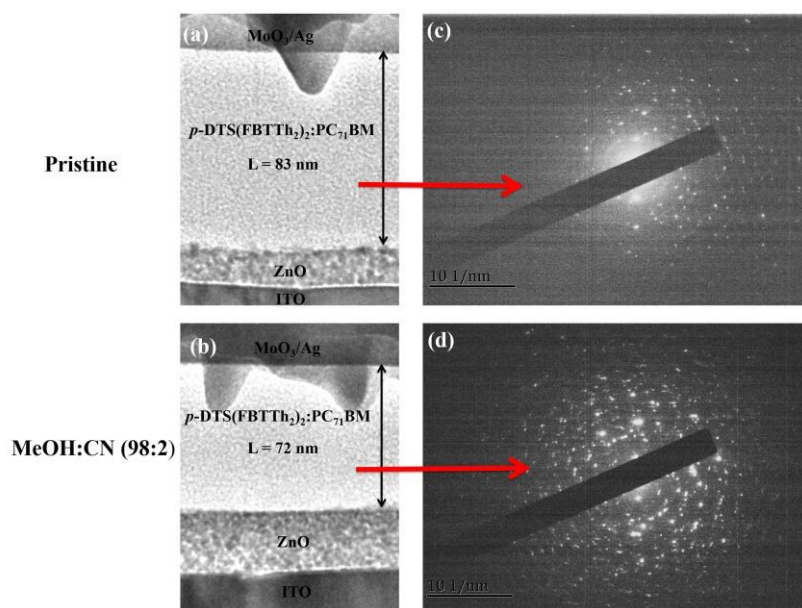
Figure 4 The cross-sectional TEM images of (a) pristine device and (b) device after treating with MeOH:CN (98:2), selected area electron diffraction of (c) pristine device and (e) device after treating with MeOH:CN (98:2).
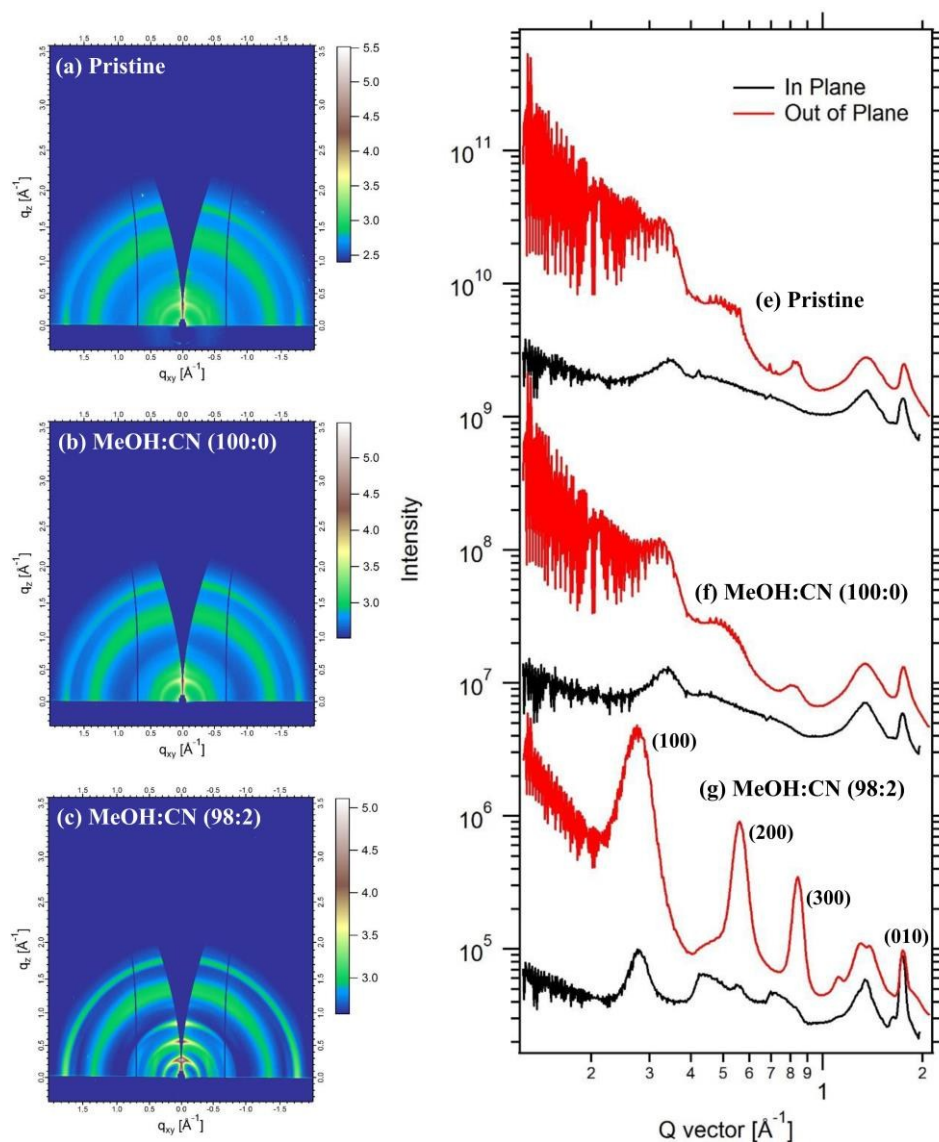
Figure 5 Two-dimensional grazing-incidence wide-angle X-ray scattering (GIWAXS) patterns (left) of (a) pristine p-DTS(FBTTh$_2$)$_2$:PC$_{71}$BM film, and films after treating by (b) MeOH solvent and (c) MeOH:CN (98:2) binary solvents. Corresponding in-plane and out-of-plane curves (right) of (e) pristine p-DTS(FBTTh$_2$)$_2$:PC$_{71}$BM film, and films after treating by (f) MeOH and (g) MeOH:CN (98:2) binary solvents.

Table 1 Solar cell device parameters with and without solvent surface treatment.

p-DTS(FBTTh$_2$)$_2$:PC$_{71}$BM	J_{sc} (mA/cm^2)	V_{oc} (V)	FF (%)	PCE (%)	μ_h ($\times 10^4$ cm^{2}V^{-1}.s^{-1})
Pristine	8.53	0.78	36.4	2.41	0.68
MeOH:CN (100:0)	8.94	0.76	36.1	2.46	0.40
MeOH:CN (99.5:0.5)	10.34	0.76	56.9	4.50	4.40
MeOH:CN (99:1)	11.08	0.77	57.7	4.90	3.60
MeOH:CN (98:2)	11.86	0.79	69.0	6.50	5.98
MeOH:CN (95:5)	10.20	0.77	49.6	3.87	5.94

Table 2 The crystal correlation length (CCL) values calculated from p-DTS(FBTTh$_2$)$_2$:PC$_{71}$BM films with and without surface solvent treatment.

p-DTS(FBTTh$_2$)$_2$:PC$_{71}$BM	pristine	MeOH:CN (100:0)	MeOH:CN (98:2)
(100)	17.1 nm	17.6 nm	25.0 nm
(010)	8.5 nm	8.5 nm	15.5 nm

Highlights

Surface Treatment by Binary Solvents Inducing Crystallization of Small Molecular Donor for Enhanced Photovoltaic Performance

Weihua Zhou, Yuanpeng Xie, Xiaotian Hu, Lin Zhang, Xiangchuan Meng, Yong Zhang, Wei Ma*, Yiwang Chen*

Surface treatment of p-DTS(FBTTh$_2$)$_2$:PC$_{71}$BM films by binary solvents of methanol and 1-chloronaphthalene enhanced PCE from 2.4% to 6.5%.

Graphical abstract